MRI Signal Formation: From Spins to Measured Signal

Bernd Müller-Bierl

April 2026

1 Introduction

Magnetic resonance imaging (MRI) is a versatile and powerful imaging modality that provides detailed insight into the structure and function of biological tissue. Unlike many other imaging techniques, MRI does not rely on ionizing radiation, but instead exploits the interaction between nuclear spins and externally applied magnetic fields.

Despite its widespread clinical use, the underlying principles of MRI are often perceived as complex, as they involve concepts from quantum mechanics, electromagnetism, and signal processing. In particular, the relation between the measured signal and the resulting image is not immediately intuitive, since spatial information is not acquired directly, but encoded in the phase and frequency of the signal.

The aim of this document is to provide a coherent and physically grounded introduction to the fundamentals of MRI. Starting from the behavior of nuclear spins in a magnetic field, the mechanisms of signal generation, relaxation, and echo formation are developed step by step. Building on this foundation, common pulse sequences and modern fast imaging techniques are introduced.

A central objective is to establish a clear understanding of spatial encoding and the concept of k-space. By linking physical intuition with a quantitative description, the reconstruction of images from measured signals is presented as a natural consequence of the underlying physics.

The presentation follows a structured progression from basic principles to more advanced imaging strategies, with the goal of making MRI both conceptually transparent and mathematically accessible.

2 Nuclear Spins and Precession

Atomic nuclei with a non-zero spin possess an intrinsic magnetic moment. In clinical magnetic resonance imaging, the relevant nuclei are primarily hydrogen nuclei (protons), which are abundant in water and fat and therefore widely distributed throughout biological tissue.

The proton carries a quantum mechanical spin, giving rise to a magnetic moment that interacts with external magnetic fields. When placed in a static magnetic field B_0, these magnetic moments preferentially align either parallel or antiparallel to the field direction.

Due to a slight energy difference between these two states, a small excess of spins occupies the lower-energy (parallel) configuration, resulting in a net magnetization along the direction of the external field.

At thermal equilibrium, a slight excess of spins occupies the lower-energy state aligned parallel to B_0 compared to those aligned antiparallel. This population difference leads to a net macroscopic magnetization vector M_0 oriented along the longitudinal (z-) direction. For an ensemble of spin-$\frac{1}{2}$ nuclei (hydrogen), the equilibrium magnetization is given by

$$M_0 = \frac{N\gamma^2\hbar^2 B_0}{4kT}, \tag{1}$$

where N is the proton density, γ the gyromagnetic ratio, $\hbar$ the reduced Planck constant, k the Boltzmann constant, and T the absolute temperature. Thus, M_0 increases with magnetic field strength and decreases with temperature. In typical MRI, however, temperature effects are small compared with the influence of B_0.

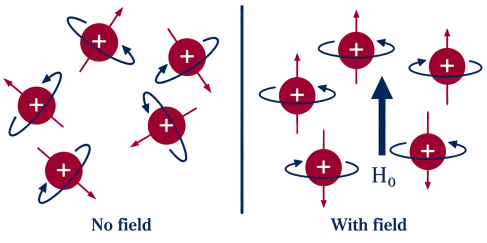

Figure 2.1: Charged particles in magnetic field diagram.

In addition to this alignment, the magnetic moments undergo precessional motion around the direction of the static magnetic field. This motion is described by the Larmor relation

$$\omega_0 = \gamma B_0, \tag{2}$$

where ω_0 is the angular Larmor frequency and γ is the gyromagnetic ratio of the nucleus, with $\gamma/2\pi = 42.58\ \text{MHz}\,\text{T}^{-1}$.

Although the behavior of individual nuclei is governed by quantum mechanics, the observable MR signal arises from an ensemble of a very large number of spins. In this regime, the net magnetization can be described by the expectation value of the spin system, which behaves according to classical equations of motion. This allows the introduction of a macroscopic magnetization vector M.

The precession of the magnetization vector is a fundamental property of magnetic resonance and determines the frequency at which the system can be excited and detected. In equilibrium, the transverse components of the magnetization cancel due to random phase distribution, and no measurable signal is observed.

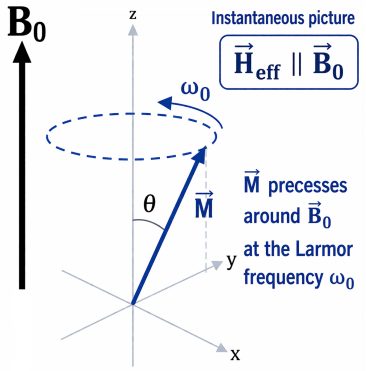

Figure 2.2: MRI vector model and precession diagram.

In the vector model, the net magnetization is represented as a vector M with longitudinal and transverse components. In equilibrium, only the longitudinal component $M_z = M_0$ is present.

The corresponding Larmor frequencies for typical clinical field strengths are summarized in Table 1.

Table 1: Larmor frequencies for typical clinical field strengths.

Magnetic Field B_0 (T)	Frequency (MHz)
1.5	64
3.0	128
7.0	298

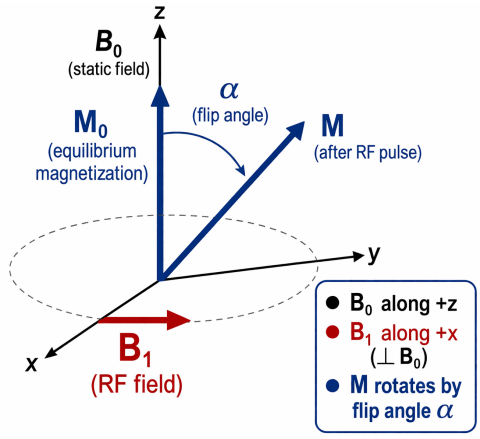

Figure 3.1: Rotation of the magnetization vector M by an RF field B_1, defining the flip angle α.

3 RF Excitation and Transverse Magnetization

An oscillating magnetic field B_1, applied perpendicular to B_0, rotates the magnetization vector away from the longitudinal direction by a flip angle α. Immediately after excitation, the spins are phase-coherent, resulting in a maximum transverse magnetization M_{xy}.

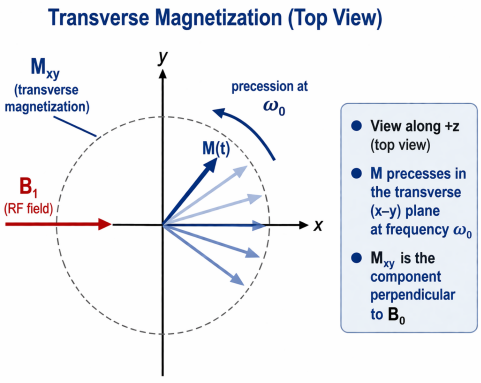

Figure 3.2: Phase coherence in the transverse plane. Immediately after RF excitation, individual spins are aligned in phase, resulting in a maximum transverse magnetization M_{xy}. The magnetization precesses at the Larmor frequency ω_0, forming the basis of the detectable MR signal.

The transverse magnetization M_{xy}, being perpendicular to B_0, induces a time-varying magnetic flux in a receive coil, giving rise to the measurable MR signal.

In practice, RF excitation and signal detection are realized by dedicated transmit and receive coils, as illustrated in Fig. 3.3.

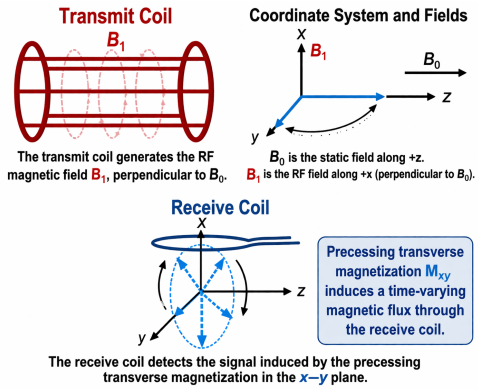

Figure 3.3: Transmit and receive coils in MRI. The RF field B_1, generated by the transmit coil, is perpendicular to B_0 and rotates the magnetization into the transverse plane. The precessing transverse magnetization M_{xy} induces a measurable signal in the receive coil.

4 Signal Formation and Dephasing

The MR signal arises from the time-varying transverse magnetization $M_{xy}(t)$ generated by RF excitation, which precesses about the static magnetic field B_0 at the Larmor frequency ω_0. This precession produces a time-varying magnetic flux through the receive coil. According to Faraday's law of induction, the changing flux induces an electromotive force, resulting in a measurable voltage $V(t)$. The detected signal reflects the transverse magnetization and oscillates at the Larmor frequency.

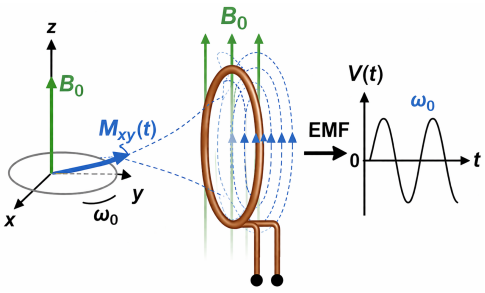

Figure 4.1: Formation and detection of the MR signal. The transverse magnetization $M_{xy}(t)$ precesses at the Larmor frequency ω_0 about the static magnetic field B_0, producing a time-varying magnetic flux in the receive coil. This induces an electromotive force (EMF) and the measured voltage $V(t)$.

After RF excitation, the transverse magnetization $M_{xy}(t)$ is initially phase-coherent, with individual spins precessing in synchrony. Over time, spin-spin interactions and magnetic field inhomogeneities lead to a progressive loss of phase coherence (dephasing), as illustrated in Fig. 4.2. As a result, the net transverse magnetization decreases, even though the magnitude of individual spins remains unchanged. This loss of coherence manifests as a decay of the measured MR signal, observed as the free induction decay (FID), which follows an exponentially damped oscillation characterized by the effective transverse relaxation time T_2^*.

This dephasing can be partially reversed by appropriate RF pulses, forming the basis of spin echo techniques.

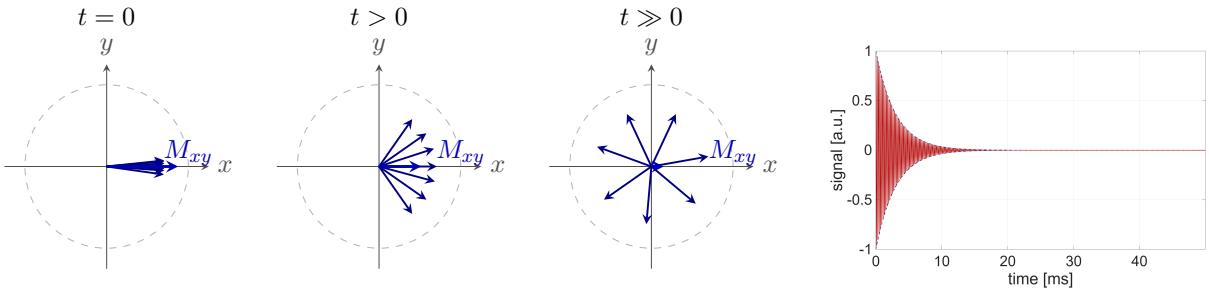

Figure 4.2: Progressive dephasing of transverse magnetization in the transverse plane and the corresponding free induction decay (FID).

5 Echo Formation (Spin Echo, Gradient Echo)

The loss of phase coherence following RF excitation can be partially reversed by applying an additional RF pulse. In a spin echo sequence, a 180° pulse is applied after a certain time, inverting the phase distribution of the spins. Spins that were precessing faster now lag behind, while slower spins move ahead.

As a result, the spins re-align in phase at a later time, leading to a temporary recovery of the transverse magnetization. This rephasing produces a measurable signal known as the spin echo.

The spin echo refocuses dephasing caused by magnetic field inhomogeneities, but not the intrinsic loss of coherence due to spin-spin interactions. Therefore, the decay of the spin echo signal is governed by the transverse relaxation time T_2, in contrast to the free induction decay, which is characterized by T_2^*.

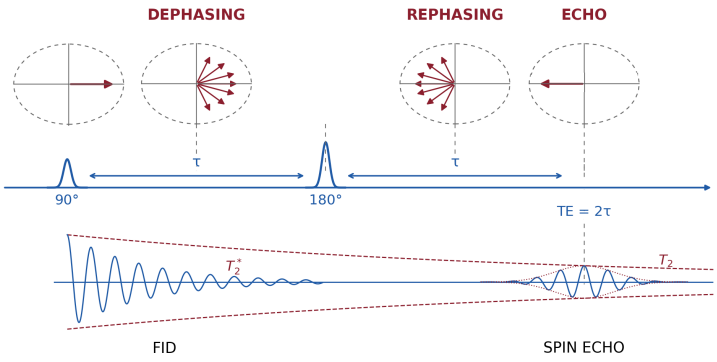

Figure 5.1: Spin echo formation by RF-induced rephasing. After a 90° excitation pulse, spins in the transverse plane progressively lose phase coherence (dephasing), leading to free induction decay (FID). A subsequent 180° pulse inverts the phase distribution of the spins, so that faster and slower spins re-align at time $TE = 2\tau$, producing a spin echo. While the spin echo refocuses dephasing caused by magnetic field inhomogeneities, it does not reverse the intrinsic transverse relaxation described by T_2.

In contrast to spin echo sequences, gradient echo techniques do not employ a refocusing RF pulse. Instead, dephasing induced by magnetic field gradients is reversed by switching the gradient polarity. However, this mechanism does not compensate for phase dispersion caused by magnetic field inhomogeneities. Consequently, the signal decay in gradient echo imaging is governed by the effective transverse relaxation time T_2^*.

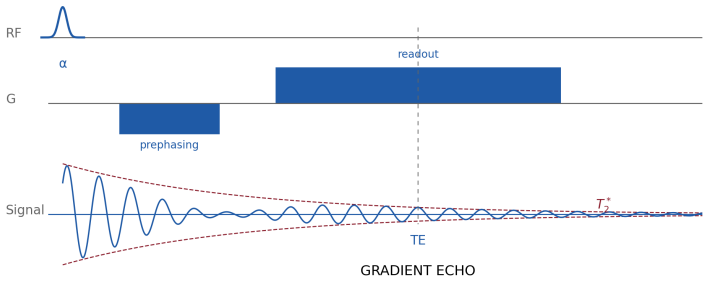

Figure 5.2: Gradient echo signal formation. Following excitation with a flip angle α, a dephasing gradient $(-G)$ introduces a controlled phase dispersion across the spins. Reversal of the gradient polarity $(+G)$ compensates this gradient-induced dephasing, leading to the formation of a gradient echo at time TE. In contrast to spin echo sequences, no refocusing RF pulse is applied; therefore, phase dispersion caused by magnetic field inhomogeneities is not reversed. Consequently, the signal evolution remains governed by the effective transverse relaxation time T_2^*.

6 Relaxation and Contrast (T_1, T_2, T_2^*)

Following RF excitation, the transverse magnetization $M_{xy}(t)$ is initially phase-coherent, with individual spins precessing in synchrony in the transverse plane. This coherent precession produces a time-varying magnetic flux through the receive coil. According to Faraday's law of induction, the changing flux induces an electromotive force, resulting in a measurable voltage signal $V(t)$ that oscillates at the Larmor frequency ω_0.

Over time, spin-spin interactions and magnetic field inhomogeneities lead to a progressive loss of phase coherence (dephasing). As a result, the net transverse magnetization decreases, even though the magnitude of individual spins remains unchanged. This loss of coherence manifests as a decay of the measured MR signal, observed as the free induction decay (FID).

The signal decay is characterized by the effective transverse relaxation time T_2^*, which includes both irreversible spin-spin interactions (described by T_2) and reversible dephasing effects due to magnetic field inhomogeneities. While T_2 reflects intrinsic tissue properties, T_2^* is additionally influenced by external field variations and is therefore shorter.

This dephasing can be partially reversed by appropriate RF pulses, forming the basis of spin echo techniques.

Longitudinal and transverse relaxation. Following RF excitation, the magnetization evolves according to two independent relaxation processes. The longitudinal magnetization M_z recovers towards its equilibrium value with a time constant T_1, whereas the transverse magnetization M_{xy} decays due to dephasing with a time constant T_2.

Tissues differ in their relaxation properties. Fat exhibits both a short T_1 and a short T_2, resulting in rapid longitudinal recovery and rapid transverse signal decay. In contrast, water shows longer T_1 and T_2 values, leading to slower recovery and more persistent transverse magnetization. These behaviors are illustrated in Fig. 6.1.

The observed transverse signal decay is influenced by two mechanisms. The intrinsic relaxation time T_2 reflects irreversible spin-spin interactions, whereas the effective relaxation time T_2^* additionally includes dephasing caused by magnetic field inhomogeneities. Consequently, $T_2^* < T_2$, as illustrated in Fig. 6.2.

Image contrast depends not only on tissue properties but also on the acquisition parameters. In a simplified spin-echo model, the signal depends on the repetition time (TR) and echo time

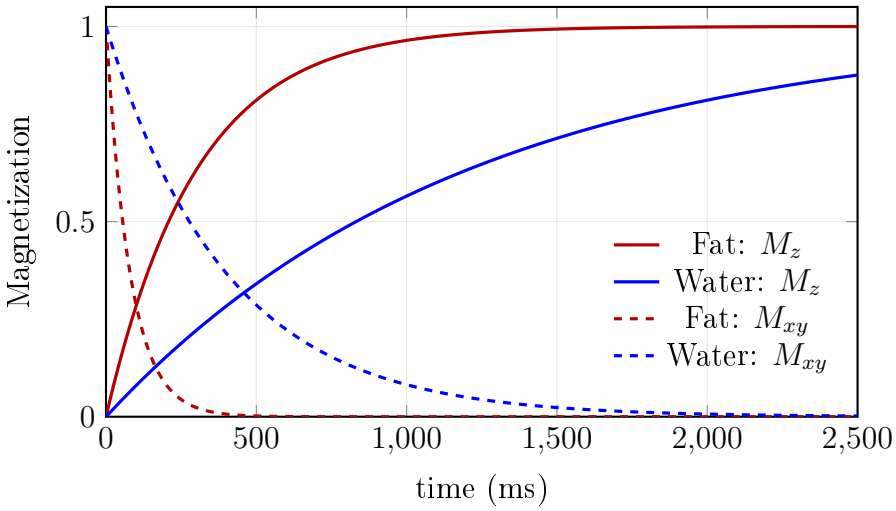

Figure 6.1: Longitudinal (T_1) and transverse (T_2) relaxation for fat and water. Solid lines represent longitudinal recovery (M_z), while dashed lines indicate transverse decay (M_{xy}).

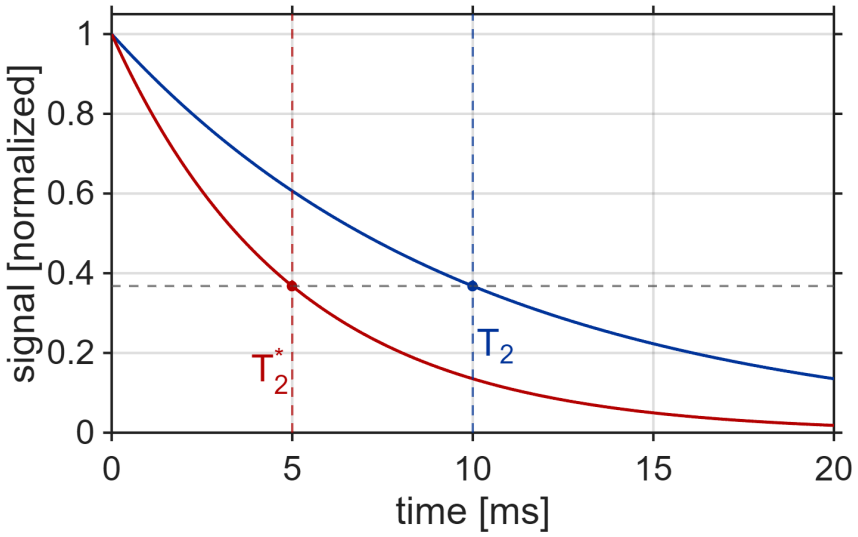

Figure 6.2: Comparison of transverse relaxation times T_2 and T_2^*. Additional dephasing due to magnetic field inhomogeneities leads to a faster signal decay characterized by T_2^*.

(TE) according to

$$S(TR, TE) \propto \rho \left(1 - e^{-TR/T_1}\right) e^{-TE/T_2}, \tag{3}$$

where ρ denotes the proton density.

Fig. 6.3 shows the dependence of the signal on TR for tissues with different T_1 values, illustrating the origin of T_1 weighting through incomplete longitudinal recovery. Fig. 6.4 displays the signal as a function of TE for different T_2 values, demonstrating how transverse decay leads to T_2 contrast.

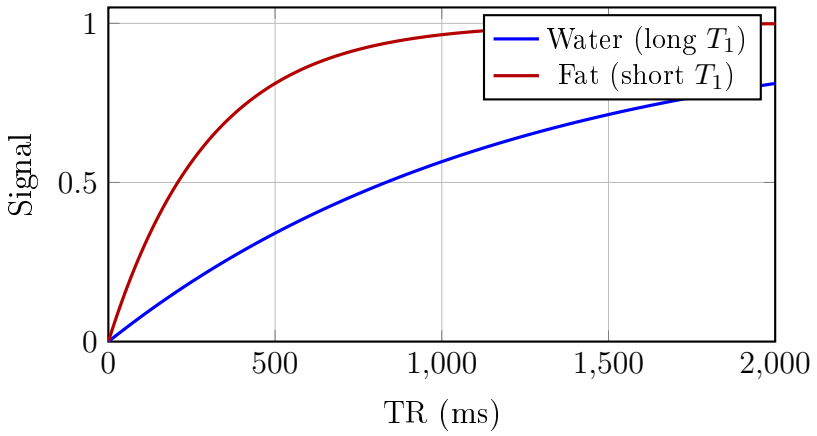

Figure 6.3: Dependence of signal intensity on repetition time (TR) for tissues with different T_1 values. Fat (short T_1) recovers more rapidly than water, leading to higher signal at short TR and thus T_1 weighting.

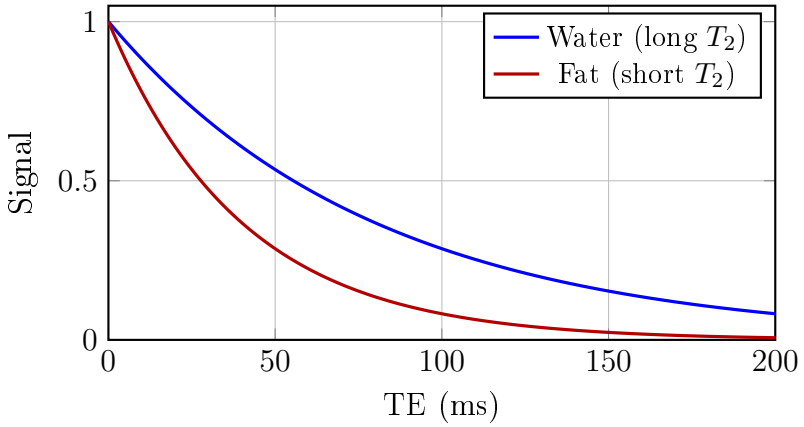

Figure 6.4: Dependence of signal intensity on echo time (TE) for tissues with different T_2 values. Water (long T_2) retains signal longer than fat, leading to T_2 contrast at longer TE.

7 Basic Sequences (SE, GRE)

Having established the physical mechanisms underlying signal formation and rephasing, these concepts can now be extended to complete imaging sequences, in which RF pulses and gradient fields are combined to encode spatial information.

7.1 Spin Echo (SE)

In spin echo sequences, a 90° RF pulse creates transverse magnetization and an oscillating free induction signal that initially decays because of T_2^* dephasing. A subsequent 180° RF pulse reverses the phase dispersion caused by static field inhomogeneities, so that the transverse signal re-grows and forms a spin echo at time TE (Fig. 7.1). Around the echo maximum, the signal is therefore governed predominantly by T_2 rather than by T_2^* effects.

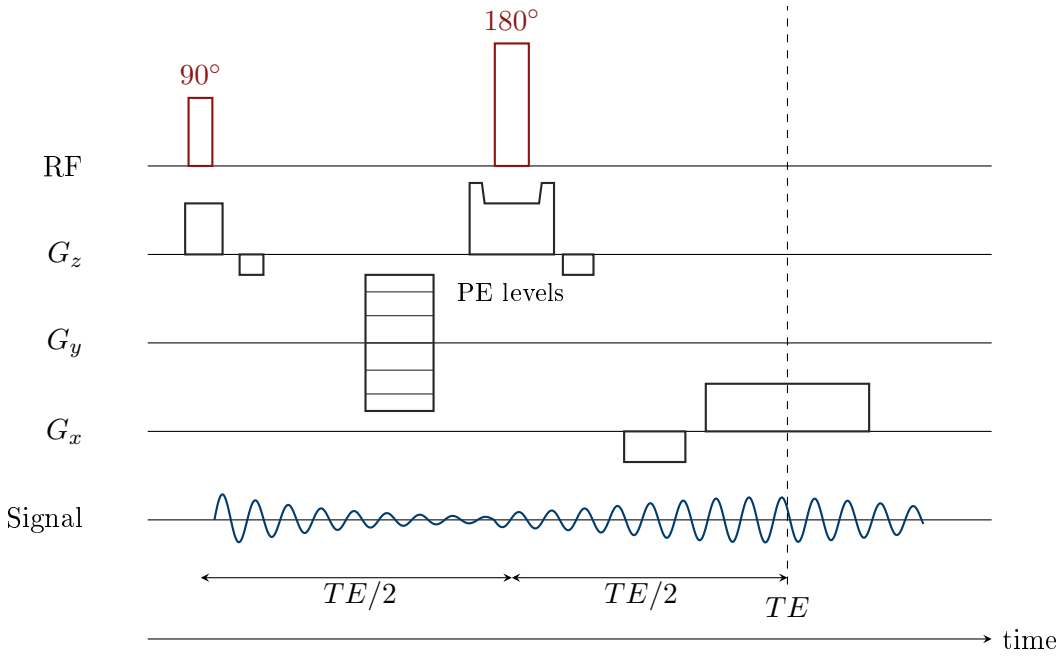

Figure 7.1: Spin echo sequence. Crusher gradients are integrated into the slice-select gradient as pronounced "longhorn" lobes around the 180° pulse, ensuring strong dephasing of unwanted coherences.

7.2 Gradient Echo (GRE)

In gradient echo sequences, the RF excitation is usually performed with a flip angle $\alpha < 90°$ during a slice-select gradient, followed by a slice-refocusing lobe of opposite polarity. No 180° refocusing pulse is applied. Instead, the readout gradient first increases dephasing and then restores phase coherence, giving rise to a gradient echo at time TE (Fig. 7.2). Because static field inhomogeneities are not removed by an RF refocusing pulse, the signal remains sensitive to T_2^* effects throughout. An adjacent spoiler gradient suppresses residual transverse coherence after readout.

In gradient-echo imaging, repeated RF excitations with short repetition times drive the magnetization into a partially saturated steady state. The signal amplitude therefore depends on both the repetition time TR and the flip angle α. For a given TR and tissue with longitudinal relaxation time T_1, there exists an optimal flip angle, known as the Ernst angle, which maximizes the steady-state signal. It is given by $\cos \alpha_E = e^{-TR/T_1}$. This concept illustrates that saturation is not merely a limitation, but can be exploited to optimize signal efficiency in rapid imaging sequences.

8 Beyond Basic Sequences

Inversion recovery sequences introduce a preparatory inversion pulse to selectively enhance T_1 contrast by controlling the recovery of longitudinal magnetization.

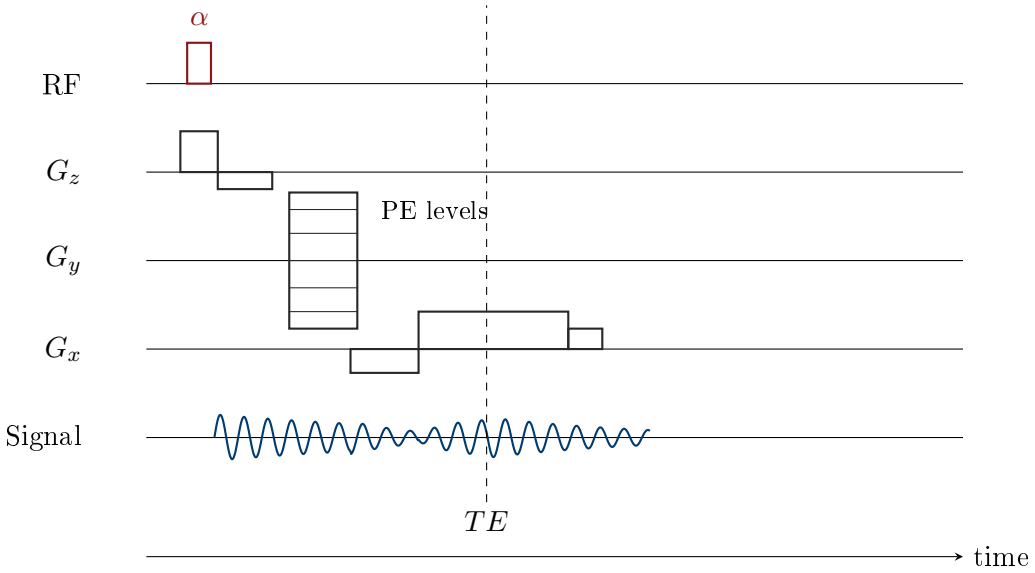

Figure 7.2: Gradient echo sequence. The flip-angle pulse α is applied during the slice-select gradient G_z, followed by a slice-refocusing lobe of opposite polarity. The readout gradient first increases dephasing and then restores phase coherence, producing a gradient echo at time TE. A small adjacent spoiler suppresses residual transverse coherence after readout. The phase-encoding gradient amplitude is varied in discrete positive and negative steps between repetitions.

Fast implementations such as FLASH use low flip angles and short repetition times to enable rapid gradient echo imaging while maintaining sufficient signal.

8.1 Steady-State Imaging (SSFP)

Steady-state free precession (SSFP) sequences are characterized by the use of short repetition times TR, such that the magnetization does not fully relax between successive RF excitations. As a result, a dynamic equilibrium is established in which both longitudinal and transverse magnetization components persist over many repetitions. The observed signal therefore arises from the continuous evolution of this steady state rather than from a single excitation.

A key distinction between different SSFP sequences lies in the treatment of transverse coherence. In unbalanced SSFP sequences (such as FISP or GRASS), residual gradient moments lead to partial dephasing of transverse magnetization between repetitions. Although a steady state is still formed, transverse coherence is only partially preserved, and the signal behavior resembles that of gradient echo imaging.

In contrast, balanced SSFP (bSSFP) fully compensates all gradient moments within each repetition. This preserves phase coherence of the transverse magnetization across successive RF pulses and establishes a fully coherent steady state. The resulting signal is highly efficient and reflects the combined influence of longitudinal recovery and transverse decay.

Because both T_1 and T_2 processes contribute continuously, the bSSFP signal exhibits a characteristic contrast that is approximately proportional to T_2/T_1. This leads to high signal intensity in tissues with relatively long T_2 and short T_1, such as fluids, and distinguishes bSSFP from conventional spin echo (T_2-weighted) and gradient echo (T_2^*-weighted) imaging.

In balanced SSFP, the RF pulses are typically applied with alternating phase (e.g., $+x$, $-x$, $+x$, ...) in the rotating frame. This phase cycling does not change the flip angle but modifies the phase reference of each excitation. As a result, residual transverse coherences evolve symmetrically over successive repetitions, stabilizing the steady state and reducing sensitivity to off-resonance effects.

Unlike spin echo or gradient echo sequences, SSFP does not create a new signal in each

repetition. Instead, the same magnetization is maintained and dynamically reshaped over time, enabling highly efficient signal generation at very short repetition times.

Table 2: Comparison of transverse magnetization behavior in different MRI sequence types.

	Spin Echo (SE)	**Gradient Echo (GRE)**	**SSFP (balanced)**
Transverse magnetization between repetitions	Refocused by 180° pulse	Dephased (spoiled) after each TR	Preserved across TRs
Refocusing mechanism	RF refocusing	Gradient reversal	Gradient balancing
Sensitivity to B_0 inhomogeneity	Reduced	High (T_2^*)	High (banding)
Signal formation	Spin echo	Gradient echo	Steady-state signal
Gradient moments per TR	Not balanced	Not balanced	Fully balanced
Use of spoilers	No	Yes (typical)	No

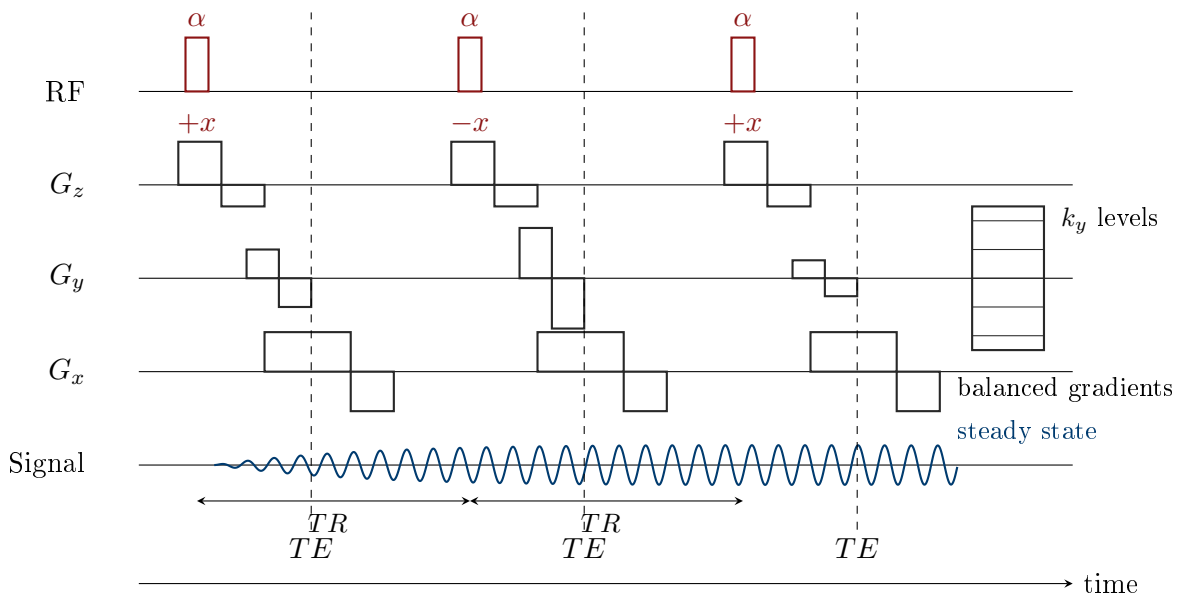

Figure 8.1: Balanced steady-state free precession (bSSFP) sequence. A rapid train of RF pulses with flip angle α establishes a dynamic steady state in which transverse magnetization persists across repetitions. All gradient moments are fully balanced within each repetition by corresponding rewinder lobes on G_x, G_y, and G_z. The signal therefore remains phase-coherent from one repetition to the next and forms a continuous steady-state oscillation rather than an isolated echo.

8.2 Ultra-Fast Imaging: Echo Planar Imaging (EPI)

Ultra-fast imaging techniques aim to acquire large portions of k-space within a single excitation. Two important realizations of this concept are echo planar imaging (EPI) and spiral imaging. In spiral imaging, k-space is traversed along a continuous spiral trajectory, improving acquisition efficiency at the cost of increased sensitivity to field inhomogeneities.

Echo planar imaging (EPI) represents a fundamentally different approach to MR image acquisition, in which a complete image (or a large portion of k-space) is acquired following a single RF excitation. This is achieved by rapidly traversing k-space using a train of echoes generated by oscillating readout gradients, thereby eliminating the need for repeated excitations for each phase-encoding step.

After a single excitation pulse, a readout gradient is rapidly switched back and forth, while small phase-encoding "blips" increment the position in the k_y direction. As a result, k-space is sampled in a zig-zag (or raster) trajectory, covering multiple lines within one repetition.

In contrast to conventional spin echo or gradient echo imaging, where each repetition samples only a single line in k-space, EPI acquires many (or all) lines within a single shot. This leads to extremely short acquisition times, enabling applications such as diffusion imaging and functional MRI (fMRI).

However, the long readout train makes EPI highly sensitive to T_2^* decay and magnetic field inhomogeneities. As a result, signal loss, geometric distortions, and susceptibility artifacts are more pronounced than in conventional sequences.

EPI can be implemented in different forms. In spin-echo EPI (SE-EPI), a 180° refocusing pulse is inserted to restore phase coherence and reduce sensitivity to magnetic field inhomogeneities, resulting in signal evolution governed predominantly by T_2 decay. In gradient-echo EPI (GE-EPI), no refocusing pulse is applied, and the signal therefore follows T_2^* decay, making it more sensitive to susceptibility effects.

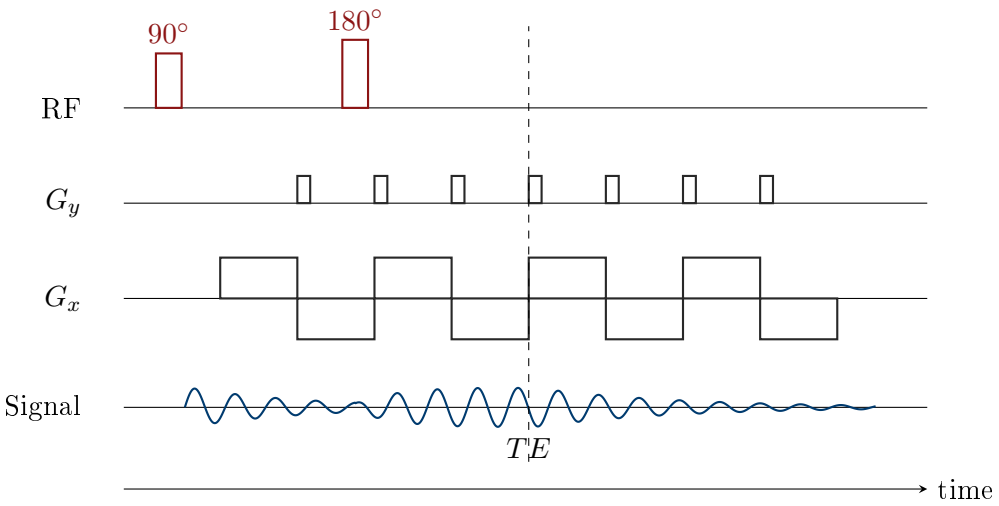

Figure 8.2: Spin-echo EPI (SE-EPI). A 180° refocusing pulse restores phase coherence, leading to a spin-echo maximum at TE. The echo train is modulated by T_2 decay rather than T_2^*, reducing sensitivity to field inhomogeneities.

In gradient-echo EPI, excitation is typically performed with a flip angle $\alpha < 90°$, commonly in the range 10°–60°, depending on sequence design and repetition time.

Spiral imaging. An alternative ultra-fast acquisition strategy is spiral imaging, in which k-space is traversed along a continuous spiral trajectory rather than line-by-line. This is achieved by simultaneously varying the two in-plane gradients, so that the readout follows a rotating trajectory through k-space after a single excitation.

In its most common implementation, spiral imaging is performed as a gradient-echo sequence with flip angle α. The resulting signal is therefore sensitive to T_2^* decay and magnetic field inhomogeneities. Because the trajectory repeatedly passes through the center of k-space, spiral imaging can achieve high acquisition efficiency and improved motion robustness compared with Cartesian echo planar imaging.

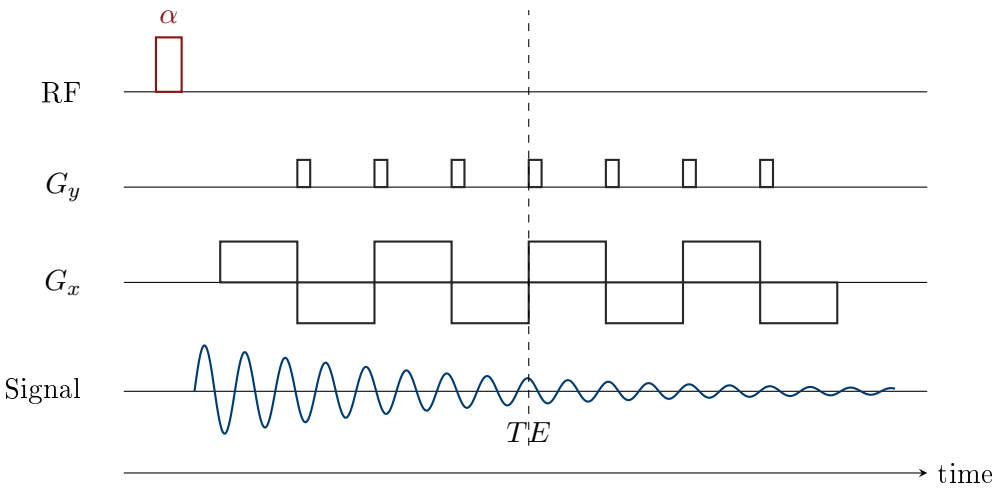

Figure 8.3: Gradient-echo EPI (GE-EPI). Following a single excitation, an oscillating readout gradient generates a train of gradient echoes while phase-encoding blips step through k_y. The signal decays continuously according to T_2^*.

However, spiral imaging requires more complex reconstruction, since the acquired data do not lie on a Cartesian grid and must be interpolated prior to Fourier transformation. Spiral imaging can also be combined with a spin-echo refocusing pulse to reduce sensitivity to field inhomogeneities, although this is less commonly used than gradient-echo spiral imaging.

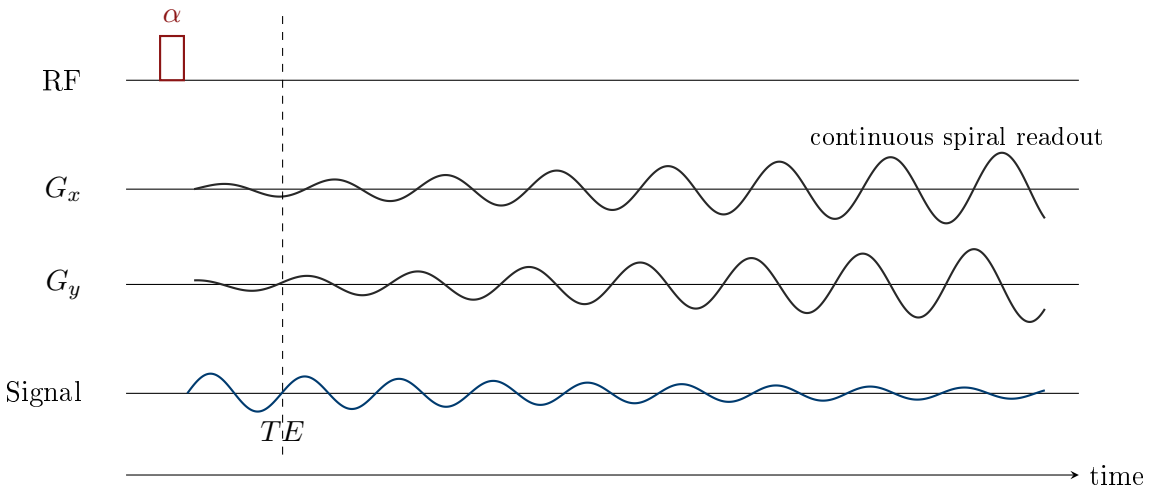

Figure 8.4: Gradient-echo spiral imaging. After excitation with flip angle α, a continuous readout is performed in which the two in-plane gradients vary smoothly and approximately in quadrature. This produces a spiral trajectory that traverses k-space from the center to the periphery within a single acquisition window. The signal is sampled continuously during this entire readout and decays according to T_2^*.

The corresponding gradient waveforms and the resulting spiral k-space trajectory are illustrated in Figs. 8.4 and 8.5.

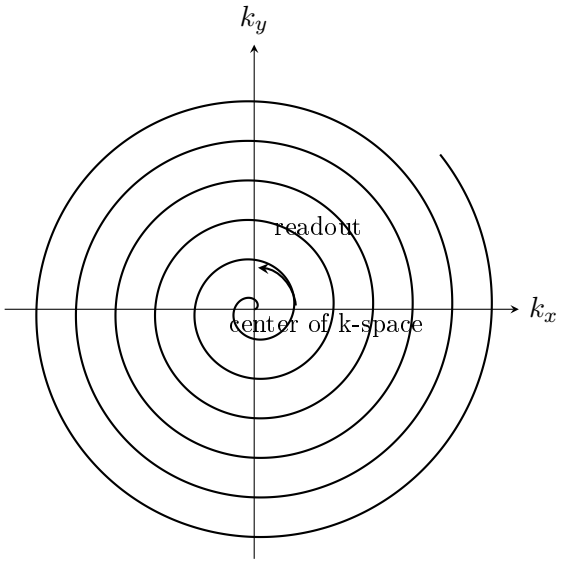

Figure 8.5: Spiral k-space trajectory. Simultaneous variation of the two in-plane gradients causes the readout to follow a continuous spiral path through k-space, beginning near the center and expanding outward so that k-space is efficiently filled.

9 Spatial Encoding

9.1 Spatial Encoding (Conceptual)

All encoding mechanisms introduced so far can be understood as specific realizations of a more general principle: the controlled accumulation of position-dependent phase in the transverse magnetization. This perspective leads naturally to the concept of k-space.

In this framework, the acquired MR signal does not directly represent spatial position, but rather a superposition of spatial frequency components.

The measured data are described in so-called *k-space*. The center of k-space contains low spatial frequencies, which determine the overall signal intensity and contrast of the image, whereas the outer regions contain high spatial frequencies, which encode fine spatial details and edges. The acquisition process can therefore be interpreted as sampling different spatial frequency components of the object.

9.1.1 Classical encoding view

In the conventional description, spatial encoding is achieved through slice selection, phase encoding, and frequency encoding gradients. Slice selection restricts the signal to a defined spatial region, while phase and frequency encoding introduce position-dependent phase and frequency shifts within the slice. By varying these gradients across repetitions and during readout, spatial information can be resolved in all three dimensions. In the more general framework, these operations correspond to sampling the spatial frequency domain (k-space).

9.2 Spatial Encoding (Mathematical Formulation)

The spatial encoding of the MR signal can be described quantitatively by considering the phase evolution of the transverse magnetization in the presence of magnetic field gradients.

In the presence of a gradient field $\mathbf{G}(t) = (G_x(t), G_y(t), G_z(t))$, the Larmor frequency becomes position-dependent:

$$\omega(\mathbf{r}, t) = \gamma \left(B_0 + \mathbf{G}(t) \cdot \mathbf{r} \right),$$

where γ is the gyromagnetic ratio and $\mathbf{r} = (x, y, z)$ denotes spatial position.

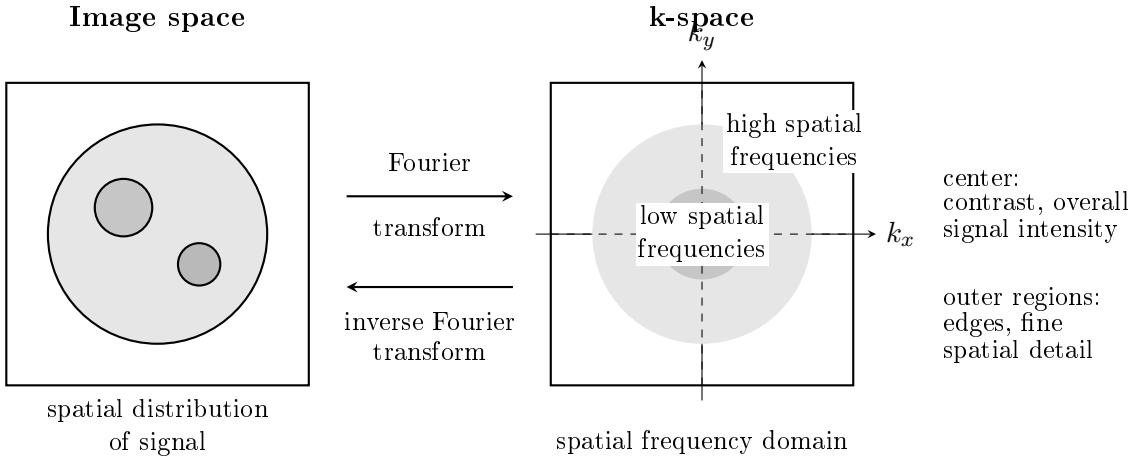

Figure 9.1: Conceptual relation between image space and k-space. The image is represented in real space by the spatial distribution of signal intensity, whereas the measured MR data are acquired in k-space, the spatial frequency domain. The center of k-space contains low spatial frequencies and primarily determines overall image contrast and signal intensity, while the outer regions contain high spatial frequencies and encode fine structural detail and edges. The image is reconstructed from k-space by inverse Fourier transformation.

The accumulated phase at time t is therefore given by

$$\phi(\mathbf{r}, t) = \int_0^t \omega(\mathbf{r}, \tau)\, d\tau = \gamma \int_0^t \mathbf{G}(\tau)\, d\tau \cdot \mathbf{r} + \gamma B_0 t.$$

The constant term $\gamma B_0 t$ does not contribute to spatial encoding after demodulation and can therefore be omitted. Defining the *k-space trajectory* as

$$\mathbf{k}(t) = \frac{\gamma}{2\pi} \int_0^t \mathbf{G}(\tau)\, d\tau,$$

the phase can be written as

$$\phi(\mathbf{r}, t) = 2\pi\, \mathbf{k}(t) \cdot \mathbf{r}.$$

The measured MR signal corresponds to the superposition of all transverse magnetization contributions:

$$s(t) = \int \rho(\mathbf{r})\, e^{i\phi(\mathbf{r},t)}\, d\mathbf{r} = \int \rho(\mathbf{r})\, e^{i2\pi \mathbf{k}(t)\cdot\mathbf{r}}\, d\mathbf{r},$$

where $\rho(\mathbf{r})$ denotes the spin density.

This expression shows that the measured signal $s(t)$ represents samples of the Fourier transform of the object $\rho(\mathbf{r})$ at positions $\mathbf{k}(t)$ in k-space. The image is therefore obtained by inverse Fourier transformation:

$$\rho(\mathbf{r}) = \int s(\mathbf{k})\, e^{-i2\pi \mathbf{k}\cdot\mathbf{r}}\, d\mathbf{k}.$$

Thus, the applied gradient waveforms $\mathbf{G}(t)$ define a trajectory $\mathbf{k}(t)$ in k-space, and the pulse sequence determines how this spatial frequency space is sampled.

10 Conclusion

Magnetic resonance imaging is based on the interplay between nuclear spin dynamics, electromagnetic fields, and signal processing. Although the individual components of this process can

be described separately, it is their combination that enables the formation of detailed images from measured signals.

Starting from the fundamental behavior of spins in a magnetic field, the mechanisms of excitation, relaxation, and signal formation lead naturally to the concept of echoes and the development of pulse sequences. Different sequence types, such as spin echo, gradient echo, and steady-state techniques, represent specific strategies for generating and manipulating the MR signal.

Modern imaging methods, including echo planar imaging and spiral imaging, demonstrate how the acquisition process can be accelerated by efficiently sampling the available signal. Despite their differences, all imaging techniques share a common principle: spatial information is encoded in the phase and frequency of the signal through the application of magnetic field gradients.

This principle is most clearly expressed in the concept of k-space, where the measured data correspond to samples of the spatial frequency content of the object. The image itself is obtained by inverse Fourier transformation, linking the physical signal formation directly to the final image representation.

Thus, MRI can be understood as a method of controlled signal encoding and reconstruction, in which the pulse sequence defines how k-space is traversed and sampled. This perspective provides a unified framework for understanding both conventional and advanced imaging techniques.